Articles

Solvothermal Elemental Direct Reaction to CdE (E = S, Se, Te) Semiconductor Nanorod

Yadong Li,* Hongwei Liao, Yi Ding, Yue Fan, Yue Zhang, and Yitai Qian

Department of Chemistry and Structure Research Laboratory,
University of Science and Technology of China, Hefei, Anhui 230026, P. R. China

Received July 27, 1998

The solvothermal reaction of sulfur, selenium, or tellurium with cadmium metal powder in different organic solvents in the temperature range 120−200 °C was investigated systematically to prepare cadmium chalcogenides, CdE (E = S, Se, Te). The results showed that the character of the products, such as crystal size, shape, and structure, were strongly influenced by the solvent and temperature during the solvothermal process. One-dimensional nanorods of CdE, with 10−40 nm diameters and several micrometers in length, were obtained by choosing coordinating solvents such as ethylenediamine and 1,6-diaminohexane as the reaction solvent. A solvent coordination molecular template mechanism for the growth of the nanorods was proposed. The CdEs thus produced were analyzed by X-ray powder diffraction, transmission electron microscopy, high-resolution electron microscopy, X-ray photoelectron spectroscopy, and elemental analysis. Ultraviolet-visible absorption, photoluminescence, and Raman spectra were used to characterize the resultant nanometer particles.

I. Introduction

The study of nanometer-sized crystallites provides an opportunity to observe the evolution of material properties with crystal structure, size, and shape.[1−4] The fabrication of nanocrystallites is an ultimate challenge of modern material research that has outstanding fundamental and potential technological consequences. How to develop the control synthesis method is always the most important goal. One-dimensional (1D) nanostructures as building blocks for many novel functional materials are currently the focus of considerable interest.[5−10] The control of nucleation and growth of 1D nanostructural material is becoming critical. The study of these mechanisms will help us to understand the chemical control synthesis of nanocrystallite nucleation and the growth process at the atomic level.

To date, considerable progress has been made in the control synthesis of II−VI family semiconductor crystallites.[11−14] These syntheses can be summed up as follows.

Ionic reaction in liquid[11]

$$MCl_2 + Na_2E \rightarrow ME\downarrow + 2NaCl$$

$$M = Cd, Zn, E = S, Se,Te$$

Gas−liquid precipitation[12]

$$M^{2+} + H_2E\ (E = S, Se, Te) \rightarrow ME\downarrow + 2H^+$$

$$M = Zn, Cd$$

Molecular precursor method[13]

$$R_2M + (TMS)_2E \rightarrow ME$$

$$M = Zn, Cd \qquad E = S, Se, Te$$

$$MR_2 + E(SiR_3)_2 \rightarrow ME$$

Electrochemical method[14]

$$Cd^{2+} + S(DMSO) \rightarrow CdS$$

All of these methods are very useful and are of widespread importance, but there are some limitations to their utilities. For examples, some methods require relatively elevated temperature,

* Corresponding author.

(1) Chen, C. C.; Herhold, A. B.; Johnson, C. S.; Alivisatos, A. P. *Science* **1997**, *276*, 398.
(2) Bawendi, M. G.; Steigerwald, M. L.; Brus, L. E. *Annu. Rev. Phys. Chem.* **1990**, *41*, 477.
(3) Motte, L.; Billoudet, F.; Laxaze, E.; Douin, J.; Pileni, M. P. *J. Phys. Chem. B* **1997**, *101*, 138. Yang, J.; Meldrum, F. C.; Fendler, J. H. *J. Phys. Chem.* **1995**, *99*, 5500.
(4) Herron, N.; Wang, Y.; Eckert, H. *J. Am. Chem. Soc.* **1990**, *112*, 1322.
(5) Dai, H.; Wong, E. W.; Lu, Y. Z.; Lieber, C. M. *Nature* **1995**, *375*, 769. Yang, P. D.; Lieber, C. M. *Science* **1996**, *273*, 1836.
(6) Yazawa, M.; Kognchi, M.; Hiruma, K. *Appl. Phys. Lett.* **1991**, 58, 1080. Yazawa, M.; Kognchi, M.; Hiruma, K. *Adv. Mater.* **1993**, *5*, 577.
(7) Wagner, R. S.; Elhs, W. C. *Appl. Phys. Lett.* **1964**, *4*, 89.
(8) Glezie, P.; Schouler, M. C.; Gradelle, P.; Caillet, M. *J. Mater. Sci.* **1994**, *29(6)*, 1576. Chang, W., et al. *Nanostructured Materials* **1994**, *4(5)*, 507. Koparanova, N.; Zlatev, Z.; Genchew, D., et al. *J. Mater. Sci.* **1994**, *29*, *103*. Toshitaka, O.; Masayuki, N. *J. Crystal Growth* **1979**, *46*, 504.
(9) Braum, P. V.; Osenar, P.; Stupp, S. I. *Nature* **1996**, *380*, 325.
(10) Trentler, T. J.; Hickman, K. M.; Goel, S. C.; Viano, A. M.; Gibbons, P. C.; Buhro, W. E. *Science* **1995**, *270*, 1791.
(11) Bandaranayake, K. J.; Wen, G. W.; Lin, J. Y.; Jing, H. X.; Sorensen, C. M. *Appl. Phys. Lett.* **1995**, *67*, 831. Wang, Y.; Herron, N. *J. Phys. Chem.* **1991**, *95*, 525.
(12) Borade, R. B. *Zeolites* **1987**, *7*, 398.
(13) Murray, C. B.; Norris, D. J.; Bawendi, M. G. *J. Am. Chem. Soc.* **1993**, *115*, 8706.
(14) Routkevitch, D.; Bigioni, T.; Moskovits, M.; Xu, J. M. *J. Phys. Chem.* **1996**, *100*, 14037.

10.1021/ic980878f CCC: $18.00
Published on Web 03/16/1999

others use toxic agents such as H_2E (E = S, Se, Te) or metalorganic compounds, or some need significant energy input. In addition, some products easily agglomerate. Above all, the morphologies of almost the produced solid semiconductor particles or small clusters are never very far from spherical particles. Studies of the rodlike II−VI family semiconductor materials, CdS nanowires,[14] and rodlike CdSe[15] prepared with electrodeposition technology have been reported. So far as we know, the realization of the chemical control synthesis of II−VI semiconductor in shape and size distribution remains difficult due to the complexity of crystal nucleation and growth process. To explore the key factor of the chemical control synthesis process, we chose different synthetic reaction systems to investigate various solvents and reaction reagents systematically. We discovered that the crystal shape, size, and structure are strongly influenced by the solvent and temperature in the solvothermal synthetic process. In this paper we present a relatively simple synthetic route for the production of high-quality samples of CdE (E = S, Se, Te) nanorod (with the emphasis on CdS) and spherical CdE (E = S, Se, Te) nanocrystallites in different solvents. Based on the experimental results, we propose a solvent-coordinating template mechanism to illustrate the formation of the CdE semiconductor nanorods. Room-temperature optical absorption and photoluminescence experiments show that the samples are of high optical quality. Transmission electron microscopy (TEM), high-resolution electron microscopy (HREM), X-ray powder diffraction (XRD), X-ray photoelectron spectroscopy (XPS), Raman spectroscopy, and elemental analysis were used to characterize the CdE (E = S, Se, Te) nanocrystallite structural features and compositions.

II. Experimental Section

Synthesis. CdE (E = S,Se,Te) compounds were synthesized by the solvothermal method.[16] Elements S (99.999%), Se (99.95%), and Te (99.95%) were stoichiometrically added with Cd powder (99.999%) to a Teflon-lined stainless steel autoclave with a capacity of 100 mL. Then the autoclave was filled with various solvents (analytical pure), such as diethylamine, ethylenediamine, glycol, benzene, pyridine, and 1,6-diaminohexane, up to about 70% of the total volume. The solution was neither shaken nor stirred during the heating period. The synthesis reaction equation is

$$Cd + E \rightarrow CdE \qquad (E = S, Se, Te)$$

The autoclave was maintained at 120−200 °C for 8−40 h and then allowed to cool to room temperature. A color precipitate was collected and washed with absolute ethanol and hot distilled water to remove residue of organic solvents. The final products were dried in a vacuum at 100 °C for 2 h. To demonstrate the influence of the solvents on crystal shape, size, and structure and further to confirm our proposed solvent-coordinating template mechanism of the CdE nanorod formation, we also used cadmium chloride ($CdCl_2 \cdot 2.5H_2O$, 99.5%) and ammonium sulfide solution $(NH_4)_2S$ (analytical pure) in different solvent and aqueous solution system to synthesize CdS, keeping the other experimental variables invariant. The purification of crystallites is the same as those already mentioned.

Structure, Composition, and Optical Property Characterization. X-ray powder diffraction (XRD) analyses were carried out on a Rigaku D/max-rA X-ray diffractometer with graphite monochromatized CuKα radiation (λ = 1.5418 Å.). The accelerating voltage was set at 50 KV, with 100 mA flux at a scanning rate of 0.05°/s in the 2θ range of 10° to 70°.

Transmission electron microscopy (TEM) spectra were taken with a Hitachi Model H-800 transmission electron microscope, with a tungsten filament, using an accelerating voltage of 200 KV. High-resolution electron microscopy (HREM) spectra were taken on a JEOL-2010 transmission electron microscope. Samples were prepared by placing a drop of dilute alcohol suspension of CdE nanocrystallites, dispersed with a supersonic disperser, onto a carbon-coated copper grid and allowing the alcohol to evaporate in the dark. Energy-dispersive X-ray fluorescence analysis (EDAX) EDAX 9100 was employed for composition determination.

X-ray photoelectron spectroscopy (XPS) spectra were recorded on a VGESCALAB MKII X-ray photoelectron spectrometer, using a nonmonochromatized MgKα X-ray as the excitation source. Raman spectra were recorded at ambient temperature with a Spex 1403 Raman spectrometer. Elemental analyses were done by traditional chemical analysis (volumetric titrimetry and gravimetric analysis) combined with atomic absorption spectroscopy using a Perkin-Elmer 1100B atomic absorption spectrophotometer. Absorption spectra were collected at room temperature on a Shimadzu ultraviolet−visible (UV−vis) absorption diode array spectrometer using 1-cm quartz cuvettes. Samples were prepared by dispersing CdE nanocrystallites in alcohol. Luminescence experiments were carried out on a Hitachi 850 fluorescence spectrometer with a Xe lamp at room temperature.

III. Results and Discussion

The solvothermal reaction to CdE using Cd metal powder with E (E = S, Se, Te) in a variety of solvents at a proper temperature yielded very interesting results. CdE semiconductor compounds were formed from Cd metal combining with nonmetals E (E = S, Se, Te) by electron transfer. Solvent and reaction temperature played a crucial role in controlling the nucleation and growth of crystallites. We made full use of these interesting results to develop the chemical control synthesis methods in crystal shape, size, and structure.

Formation of Nanorods. First, a series of solvothermal synthetic experiments with 0.01 mol Cd powder and 0.01−0.011 mol S, which was 10% excess of the calculated amount, were carried out in various solvents, such as diethylamine, ethylenediamine, glycol, pyridine, benzene and 1,6-diaminohexane, at 200 °C. When glycol and benzene were used as the solvothermal synthetic solvent, there was no CdS formed among the products. The product from the reaction was inhomogeneous and consisted of the unreacted metal powder and E (S, Se, and Te). Only in strongly coordinating alkylamine solvents, such as diethylamine, ethylenediamine, pyridine, and 1,6-diaminohexane, were the obtained products CdS. These products were confirmed by XRD (Figure 1), EDAX, element analysis, and XPS (Figure 2) results. Obvious differences in crystal size, shape, and structure are evident in the XRD patterns of the samples produced in four kinds of coordinating alkylamine solvents (Figure 1). Figure 1A, the XRD pattern of the sample produced in ethylenediamine, shows that the obtained sample is a pure hexagonal CdS phase (wurtzite structure) with lattice constants a = 4.136 and c = 6.713 Å (equal to the values of JCPDS 6-314). However, there is a bit stronger (002) peak in the XRD pattern than expected from the powder pattern, which indicates a preferential orientation of [001] in the CdS crystal. We inferred that the CdS crystal growth was oriented and morphologies were 1D rodlike. This inference was confirmed by TEM images (Figure 3A). The CdS crystallites display rodlike monomorphology with a size of 500−1000 × 20−40 nm. HREM is used to detect the fine structure of the CdS nanorods. Figure 3I shows a typical image of a 20-nm diameter CdS nanorod. The (002) lattice fringes of CdS in the wurtzite structure appear frequently, indicating the preferential orientation of the rodlike CdS particles.

(15) Minoura, H.; Negoro, T.; Kitakata, M.; Ueno, Y. *Sol. Energy Mater.* **1985**, *12(5)*, 335−344.

(16) Li, Y. D.; Duan, X. F.; Qian, Y. T.; Yang, L.; Ji, M. R.; and Li, C. W. *J. Am. Chem. Soc.* **1997**, *119*, 7869. Li, Y.D.; Duan, X. F.; Liao, H. W.; Qian, Y. T. *Chem. Mater.* **1998**, *10*, *0(1)*, 48.

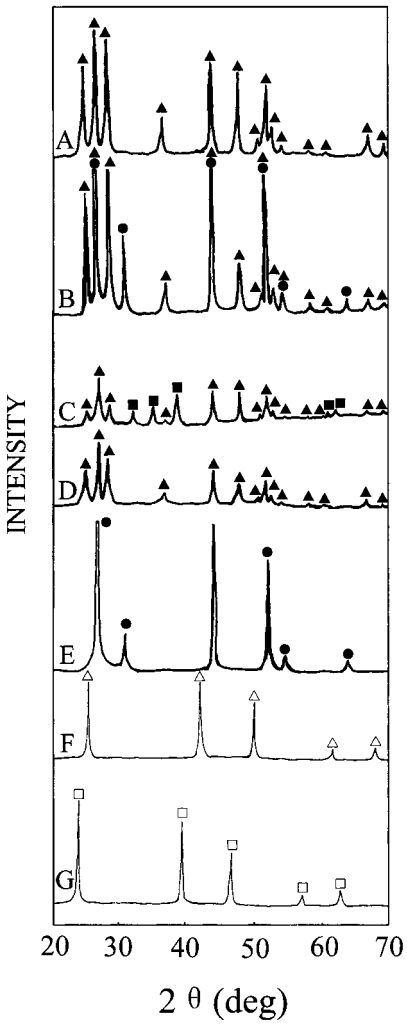

Figure 1. XRD patterns of the samples: (A) CdS in ethylenediamine (Cd + S); (B) CdS in diethylamine (Cd + S); (C) CdS in pyridine (Cd + S); (D) CdS in 1,6-diaminohexane (Cd + S); (E) CdS in water ($CdCl_2$ + $(NH_4)_2S$); (F) CdSe in ethylenediamne (Cd + Se); (G) CdTe in ethylenediamine (Cd + Te). Key: (▲) hexagonal CdS; (●) cubic CdS; (■) Cd; (△) CdSe; (□) CdTe).

Figure 1B is the XRD pattern of the sample produced in diethylamine, which shows that two CdS phases exist: a hexagonal phase, with lattice constants $a = 4.136$ and $c = 6.713$ Å, and a cubic phase, with lattice constant $a = 5.818$ Å (zinc-blend structure). The TEM image (Figure 3B) shows that the morphology of the CdS crystallites is spherical and the average particle size is about 20 nm.

Figure 1C is the XRD pattern of the sample produced in pyridine. All the reflections can be indexed to be a pure hexagonal phase with lattice constants $a = 4.136$ and $c = 6.714$ Å, which are near the reported values.[3] There is a bit stronger (002) peak in the pattern than expected. But the TEM image (Figure 3C) shows that CdS crystal growth in pyridine was not oriented. The morphology of the CdS crystallites is spherical and the average particle size is about 50 nm.

Figure 1D is the XRD pattern of the sample obtained in 1,6-diaminohexane. All the peaks can be indexed to the hexagonal phase, with lattice constants $a = 4.137$ and $c = 6.714$ Å. These results are analogous to those in Figure 1A. There is a bit stronger (002) peak in the pattern than expected from the powder pattern, which indicates a preferential orientation of [001] in nanocrystalline CdS. This orientation was confirmed by the

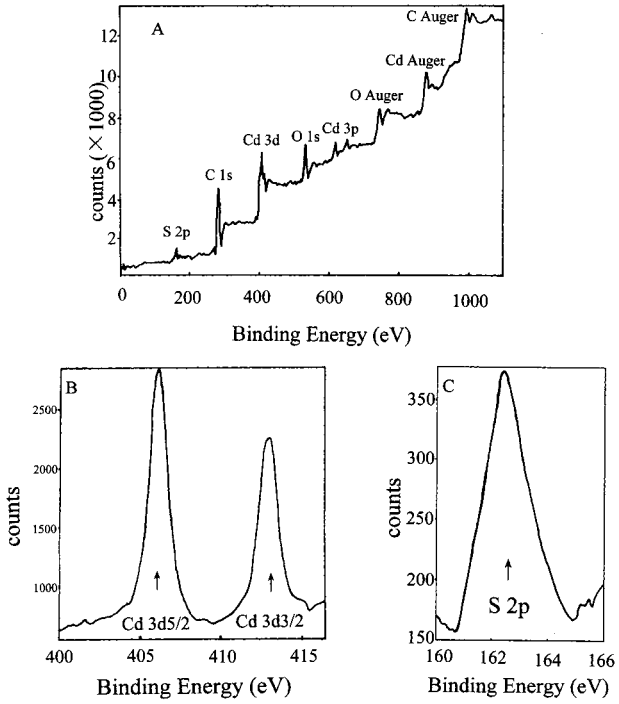

Figure 2. XPS spectra of CdS nanorods: (A) typical XPS survey spectrum of CdS nanorods; (B) close-up surveys for Cd 3*d* core; (C) close-up surveys for S 2*p* core.

TEM image (Figure 3D) in which the nanocrystalline CdS displayed rodlike monomorphology with a size of 120−600 × 10−20 nm.

To illustrate the interesting results just reported, we proposed a solvent coordinating molecular template mechanism. At room temperature, metal Cd powder can react with sulfur ethylenediamine solution. XRD analysis showed that the obtained white powder is neither CdS nor Cd, but is the complex of $[Cd(en)_2]^{2+}$ (the stability constants, $\log \beta_2 = 10.09$), which is confirmed by IR spectroscopy. With the increase of the temperature, the stability of the complexes decreased. At relatively elevated temperature (e.g., >120 °C), S may connect the aforementioned complexes to form 1D structure CdS nanorods and the volatile coordinated ligands are gradually lost. In previous work, Rauchfuss and co-workers reported that Zn reacts with S in a strongly coordinating solvent (*N*-methylimidazole) and forms complexes of the form $ZnS_6(N\text{-MeIm})_2$,[17] which is analogous to our results. In our work, during the process of the CdS formation, this bidentate ligand complex served as an intermediate in the control of the CdS crystal growth. CdS is the result of the competition of the following two reactions:

$$Cd + S \rightarrow CdS \rightleftharpoons Cd^{2+} + S^{2-} \quad (1)$$

$$Cd(en)_2^{2+} \rightleftharpoons Cd^{2+} + 2en \quad (2)$$

However, in pyridine or diethylamine, the solvent molecules can also form complexes with Cd^{2+}, but the stability ($\log \beta_4 = 2.50$) of the complex is much lower than that of former complex. The CdS formation reaction in these solvent systems is relatively easy, so the epitaxial growth of the CdS crystal is difficult to be realized.

To further understand the solvent coordinating molecular template mechanism just proposed, we needed to obtain more

(17) Dev, S.; Ramli, E.; Rauchfuss, T. B.; Wilson, S. R. *J. Am. Chem. Soc.* **1990**, *112*, 6385.

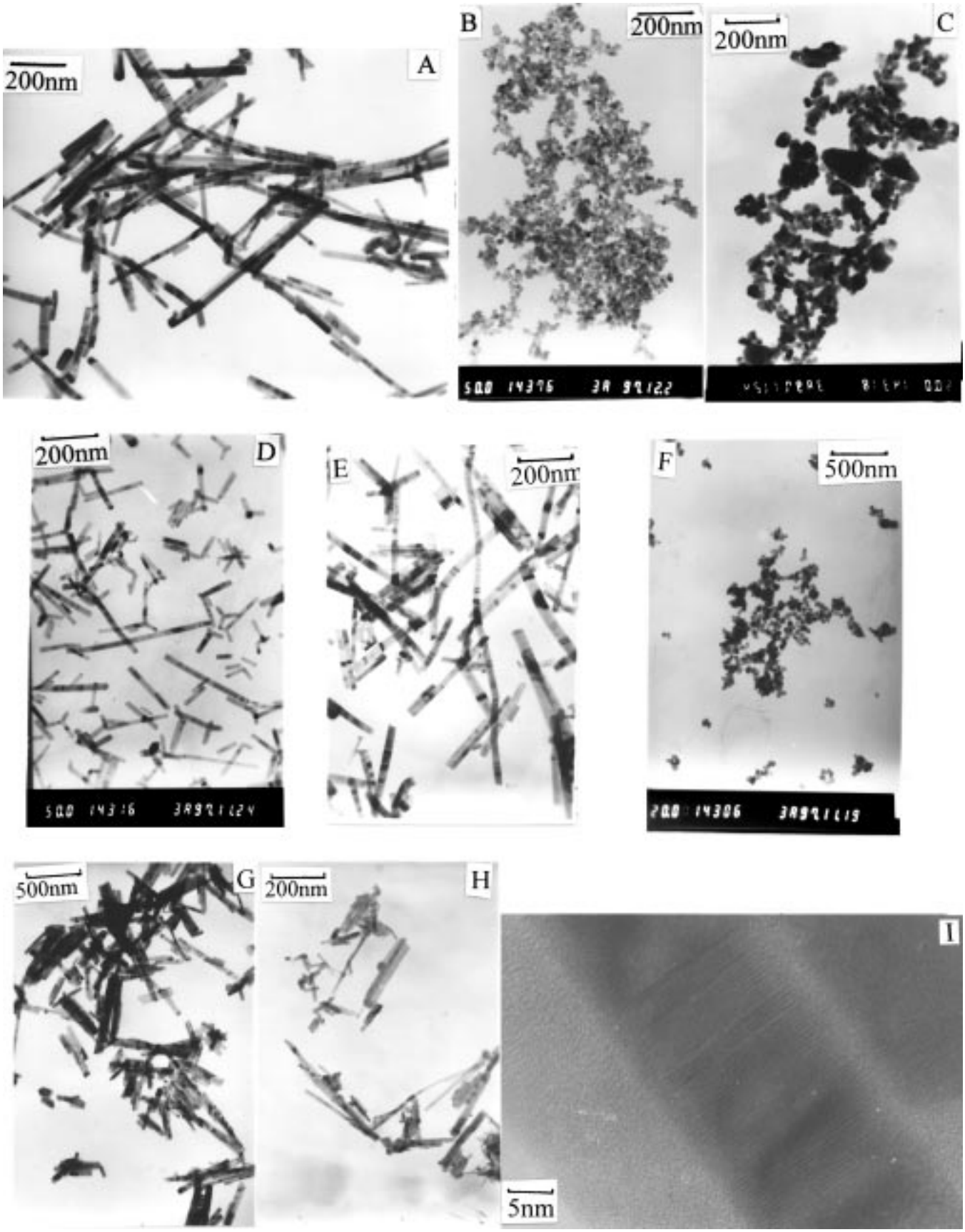

Figure 3. TEM and HREM images of the samples: (A) CdS in ethylenediamine (Cd + S); (B) CdS in diethylamine (Cd + S); (C) CdS in pyridine (Cd + S); (D) CdS in 1,6-diaminohexane (Cd + S); (E) CdS in ethylenediamine ($CdCl_2$ + $(NH_4)_2S$); (F) CdS in water ($CdCl_2$ + $(NH_4)_2S$, 150C); (G) CdSe in ethylenediamine (Cd + Se); (H) CdTe in ethylenediamine (Cd + Te); (I) HREM image of CdS in ethylenediamine (Cd + S).

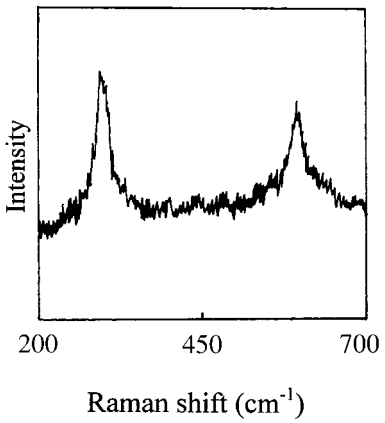

Figure 4. Raman spectrum of CdS nanorods.

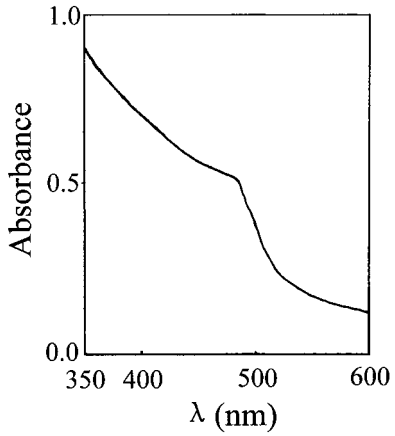

Figure 5. UV−vis absorption spectrum of CdS nanorods.

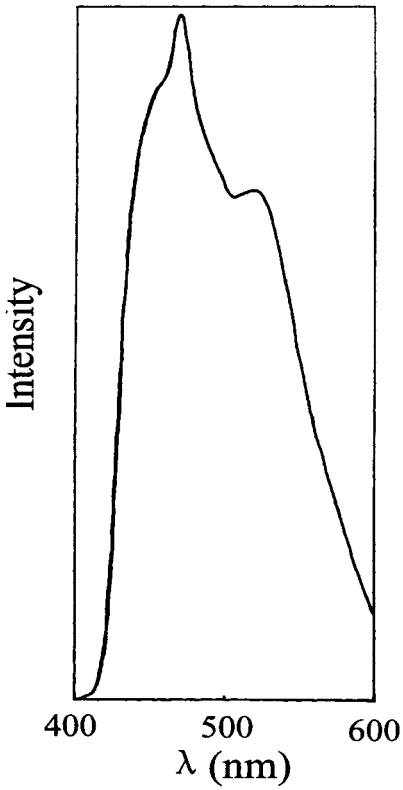

Figure 6. Photoluminescence spectrum of CdS nanorods.

experiment results to support it. For this purpose, we designed a series of related experiments to test the mechanism. First, we chose $CdCl_2$ and $(NH_4)_2S$ as reactants to synthesize CdS at 120 °C in different solvents, such as water, ethylenediamine, and pyridine. The results indicated that only in ethylenediamine were the CdS nanorods with size 200−1200 × 10−50 nm obtained (Figure 3E), but the morphology of the CdS samples in water (Figure 3F) and pyridine were spherical. It is noteworthy that the CdS sample obtained in water is a pure cubic Zn-blend structure with lattice constant $a = 5.818$ Å (Figure 1E). Second, we used elements Se and Te to substitute for S in the Cd powder reaction in ethylenediamine and pyridine, respectively at 200 °C to synthesis CdE (E = Se, Te). The results indicated that although the obtained samples, CdSe and CdTe in ethylenediamine, were both cubic Zn-blend structure phases (Figures 1F and 1G), both of them displayed rodlike morphology (Figure 3G and 3H). However, the obtained samples in pyridine really showed spherical morphology. These experimental results further support the proposed solvent coordinating molecular template mechanism. This method may be applicable to synthesize other 1D inorganic nanometer materials. Further studies on the solvent coordinating molecular template mechanism are in progress.

X-ray Photoelectron Spectrum (XPS). XPS was carried out to derive composition information about the obtained samples (Figure 2). Figure 2A is the typical survey spectrum of CdS nanorods, showing the presence of Cd, S from the nanorods and their surface, and C and O from the surface of the nanorods and from the absorbed gaseous molecules.

Higher-resolution spectra were taken of the Cd and S regions of samples as prepared (Figure 2B). The two strong peaks at 162.50 and 406.15 eV correspond to S(2p) and Cd(3d) binding energy, respectively, for CdS. No obvious other peak was observed. The scans show no evidence of peaks other than Cd and S core from the main and satellite Mg X-ray. There was no evidence of shake-up peaks, which are photoemission peaks from species ionized prior to the observed photoemission process and generally occur several electronvolts higher than the binding energy of the main peaks in the spectra.

Peak areas of the Cd and S cores were measured and used to calculate the Cd-to-S ratio for the nanorods. Areas were determined by fitting each of the curves using a nonlinear least-squares curve-fitting program[18] and taking the area of the fit peak. Because the shape of the background was uncertain, the absolute areas are accurate to an error of about 12%. However, the background is kept the same for all fits, so the relative error is much smaller. An empirical correction was made for the pass energy variation between two scans when there was a difference. The quantification of the peaks gives a Cd-to-S ratio of 1.05:1. Elemental analysis shows a Cd-to-S ratio of 1.07. These results were identical.

Raman Spectroscopy (RS). Raman spectroscopy (RS) (Figure 4) was used to characterized the obtained CdS sample. Figure 4 shows that the spectrum is dominated by overtones of the longitudinal optical phonon (LO). The CdS nanorods produced a Raman spectrum with two clearly discernible LO modes. A strong overtone progression of long wavelength longitudinal optical vibration manifests in the laser Raman spectrum, which may be caused by a lattice deformation produced by electronic excition in bulk CdS.[19] Strong Raman spectra could be analyzed to yield values of the band gap and the homogeneous line width of the excited state. The Raman

(18) Peakfit viersion 3.10; Jandel Scientific, 1992.

(19) Klein, M. L.; Porto, S. P. S. *Phys. Rev. Lett.* **1969**, *22*, 782. Scott, J. F.; Leite, R. C. C.; Damen, T. C. *Phys. Rev.* **1969**, *188*, 1285.

spectrum possesses a background signal that increases with increase of Raman frequency. The background was due to luminescence originating from the CdS nanorod. The intensity and the number of the overtone depend on both the value of the band gap and the displacement of the minimum of the ground state along the normal mode of the crystal corresponding to the LO phonon.[20] Here, we observed only two overtones in the Raman spectrum in the range 200−700 cm^{-1}, which is consistent with that in the literature.[21]

Optical Properties. The UV−vis absorption spectra of the obtained CdS nanorods samples are shown in Figure 5. The absorption band yielded an onset near 520 nm and absorption peak at 480 nm, which is the characteristic absorption band of CdS. This result is consistent with the characteristic absorption of bulk CdS. We did not observe the UV−vis absorption of CdSe and CdTe nanorods.

The photoluminescence (PL) spectrum, shown in Figure 6, used an excitation at 370 nm with a 430-nm filter. It is noteworthy that the PL spectrum shows a intense, sharp PL peak at 467 nm with two shoulder peaks at 452 and 518 nm. The literature[22] reported that the recombination of excitons and/or shallowly trapped electron/hole pairs causes the band edge luminescence (narrow bands between 450 and 500 nm). These PL emissions indicate that, after light absorption in the CdS nanorods, the photogenerated electron/hole pair was trapped, with emission at 467 nm upon their recombination. Only a small fraction of excitons (or weakly trapped electron/hole pairs) produced 452-nm photons without apparent stokes shift. The 518 nm emission is the characteristic emission of the bulk CdS.

Conclusion

A novel solvothermal synthetic route to CdE (II−VI) semiconductor nanorods has been developed. The reaction conditions in this route are very easy to maintain and control. By merely choosing different solvents and temperature, we can obtain different target products in crystal size, shape, and structure.

A new solvent coordination molecular template mechanism for growth of the nanorod is proposed. It may be applicable to synthesize other 1D inorganic nanometer materials.

Acknowledgment. This work is supported by the National Natural Science Foundation of China and the National Nanometer Materials Climbing Project.

IC980878F

(20) Routkevitch, D.; Bigioni, T.; Moskovits, M.; Xu, J. M. *J. Phys. Chem.* **1996**, *100*, 14037.

(21) Shiang, J. J.; Goldstein, A. N.; Alivisatos, A. P. *J. Chem. Phys.* **1990**, *92(5)*, 3232.

(22) Spanhel, L.; Anderson, M. A. *J. Am. Chem. Soc.* **1990**, *112*, 2278.